

## Supplementary Materials

### Catalytic activity of silicon nanowires decorated with gold and copper nanoparticles deposited by pulsed laser ablation

Michele Casiello,<sup>1</sup> Rosaria Anna Picca,<sup>1</sup> Caterina Fusco,<sup>2</sup> Lucia D'Accolti,<sup>1,2</sup> Antonio Alessio Leonardi,<sup>3,4</sup> Maria Josè Lo Faro,<sup>3</sup> Alessia Irrera,<sup>3</sup> Sebastiano Trusso,<sup>3</sup> Pietro Cotugno,<sup>1</sup> Maria Chiara Sportelli,<sup>1</sup> Nicola Cioffi,<sup>1,\*</sup> Angelo Nacci,<sup>1,2,\*</sup>

#### Contents:

XPS analyses (Tables S1-S3 and Figures S1-S3) .....	page 2
Optimization of C <sub>aryl</sub> -N coupling conditions (Table S4) .....	page 5
Evaluation of TON and TOF values.....	page 6
MS data of reaction products .....	page 7
References .....	page 12

### XPS analyses

Typical surface composition and relevant regions for Au and Cu nanocomposites are reported below:

**Table S1.** Typical surface composition as determined by XPS analysis on AuNP-decorated materials, expressed in terms of element atomic%, error on gold percentage is  $\pm 0.2\%$ ; error on the other elements is  $\pm 0.5\%$

SAMPLE	C%	Au%	Si%	O%
<b>AuNPs@SiNWs</b>	44.2	40.6	3.6	11.6
<b>Au@Si bulk</b>	56.9	24.3	< 0.5	18.8

**Table S2.** Typical surface composition as determined by XPS analysis on CuNP-decorated materials, expressed in terms of element atomic%, error on copper percentage is  $\pm 0.2\%$ ; error on the other elements is  $\pm 0.5\%$

SAMPLE	C%	Cu%	Si%	O%
<b>CuNPs@SiNWs</b>	36.3	10.5	18.0	35.2
<b>Cu@Si bulk</b>	61.2	3.3	3.3	27.2

**Table S3.** Typical surface composition as determined by XPS analysis on used AuNP- and CuNP-decorated SiNWs, expressed in terms of element atomic%, error on gold and copper percentages is  $\pm 0.2\%$ ; error on the other elements is  $\pm 0.5\%$

SAMPLE	C%	Au% or Cu%	Si%	O%	K%	N%	Mg%
<b>Used AuNPs@SiNWs</b>	55.2	0.5	10.0	30.7	1.0	2.6	< 0.2
<b>Used CuNPs@SiNWs</b>	17.3	0.5	37.7	43.4	< 0.1	1.1	-

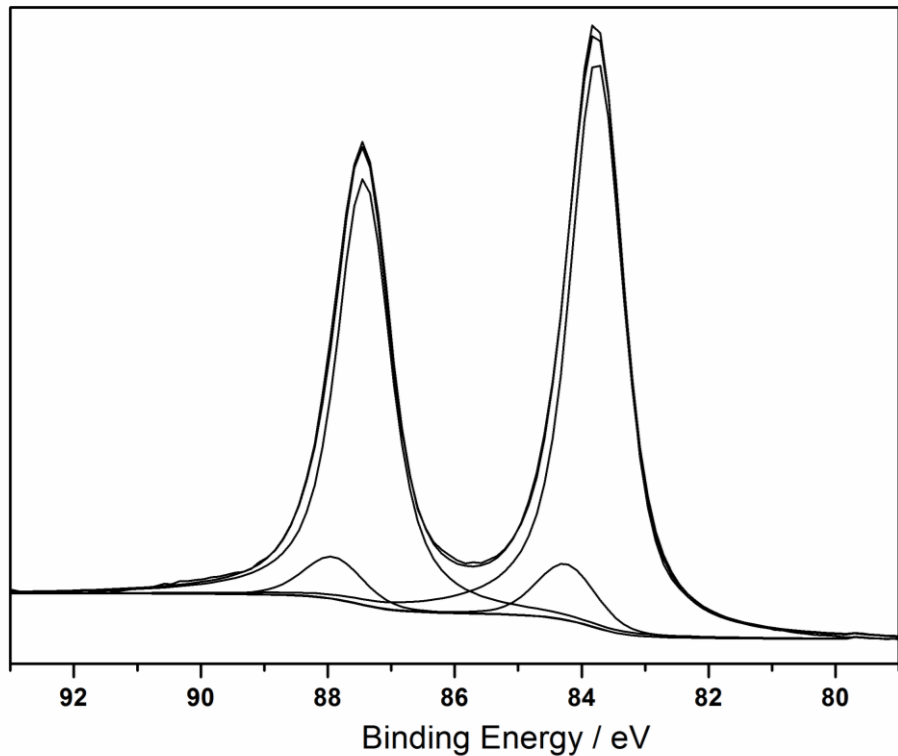


**Figure S1.** Au4f region relevant to Au@Si<sub>bulk</sub> sample.

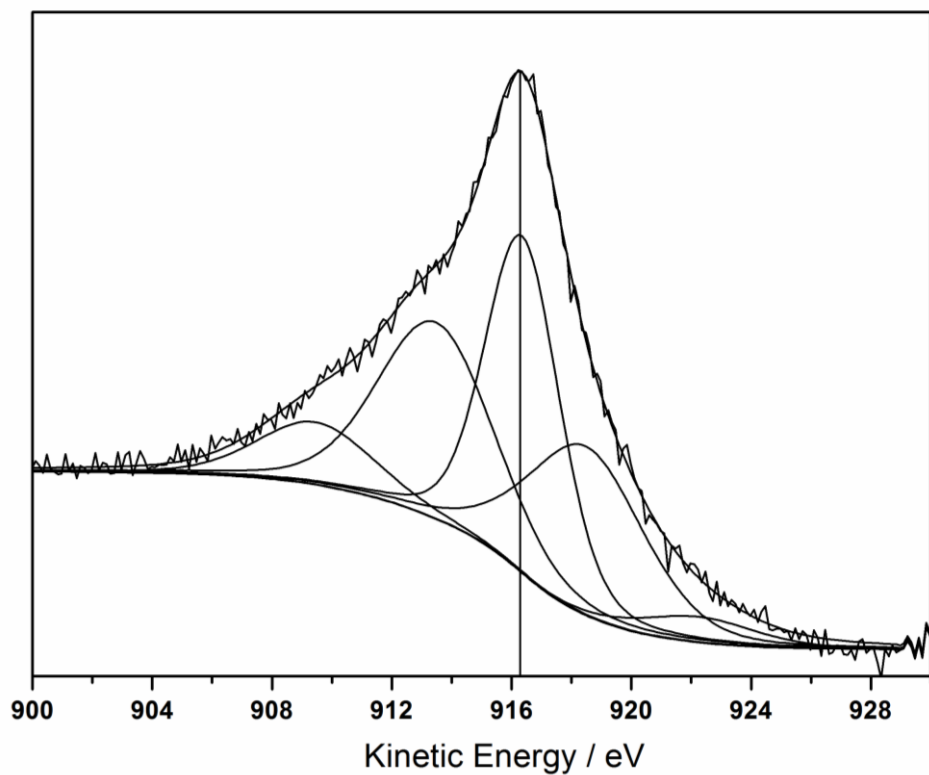


**Figure S2.** CuL<sub>3</sub>M<sub>45</sub>M<sub>45</sub> Auger region relevant to CuNPs@SiNWs. The line indicates the KE<sub>CuLMM</sub> used to calculate  $\alpha'$ .

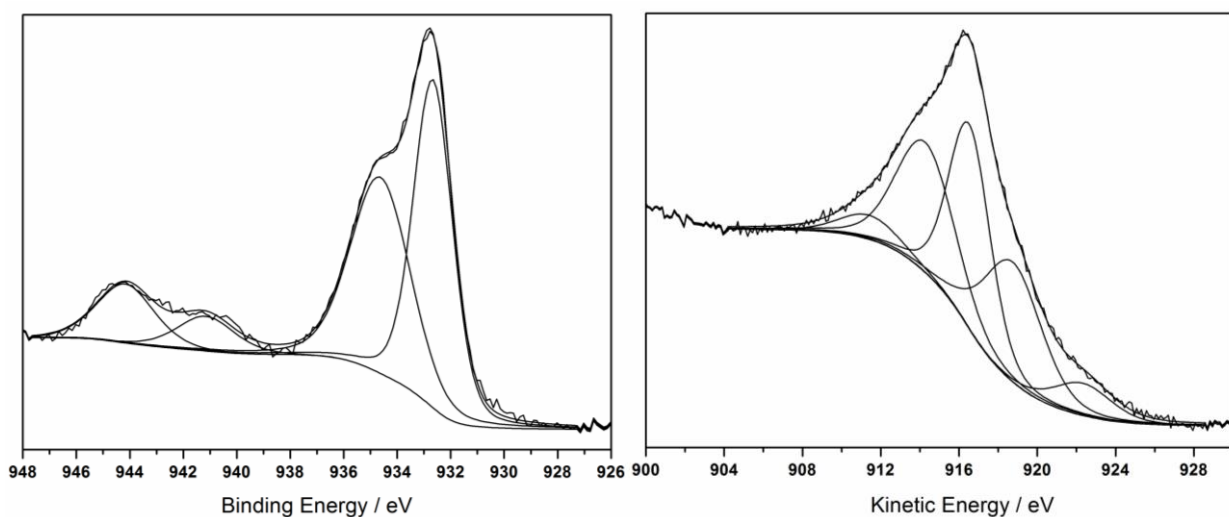


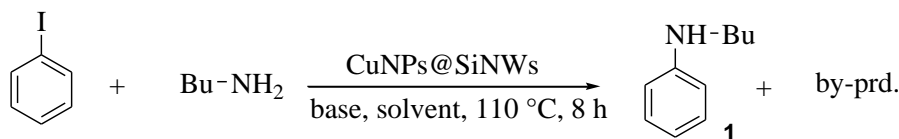
**Figure S3.** Cu2p<sub>3/2</sub> (left) and CuL<sub>3</sub>M<sub>45</sub>M<sub>45</sub> (right) regions relevant to CuNPs@Si<sub>bulk</sub>.

### Optimisation of coupling Caryl-N coupling conditions

Caryl-N coupling conditions were optimised on the model reaction between iodobenzene and butylamine promoted by CuNPs@SiNWs as the catalyst. Among the several bases investigated, Cesium carbonate provided the best performances (Table S4, runs 1-5); while water was the most efficient reaction medium most probably due to both the good solvent ability towards  $\text{Cs}_2\text{CO}_3$  and the worse nucleophilic properties than amine that suppressed the competitive side-reaction of hydrolysis affording phenol (Table S4, runs 5-11).

Heating affected the coupling in a predicted manner: temperatures below 110 °C afforded modest yields, whereas higher temperature decreased selectivity (table S4, runs 12-13).

**Table S4.** Optimisation of C-N coupling conditions catalysed by Cu-NP@SiNWs.<sup>a)</sup>



Run	Solvent	Base	Conv. <sup>b)</sup> (%)	Sel. (%) <sup>b)</sup>	
				<b>1</b>	by-prd
1	$\text{H}_2\text{O}$	-	5	-	
2	$\text{H}_2\text{O}$	$\text{NEt}_3$	10	82	18
3	$\text{H}_2\text{O}$	$\text{Bu}_4\text{NOAc}$	15	66	34
4	$\text{H}_2\text{O}$	$\text{K}_2\text{CO}_3$	75	88	12
5	$\text{H}_2\text{O}$	$\text{Cs}_2\text{CO}_3$	98	96	4
6	$\text{CH}_3\text{CN}$	$\text{Cs}_2\text{CO}_3$	75	91	9
7	DMF	$\text{Cs}_2\text{CO}_3$	20	85	15
8	DMSO	$\text{Cs}_2\text{CO}_3$	10	-	
9	THF	$\text{Cs}_2\text{CO}_3$	20	78	22
10	DMA	$\text{Cs}_2\text{CO}_3$	<5	-	
11	$\text{H}_2\text{O}/\text{CH}_3\text{CN}^{\text{c})}$	$\text{Cs}_2\text{CO}_3$	40	95	5
12 <sup>d)</sup>	$\text{H}_2\text{O}$	$\text{Cs}_2\text{CO}_3$	45	86	14
13 <sup>e)</sup>	$\text{H}_2\text{O}$	$\text{Cs}_2\text{CO}_3$	100	52	48

<sup>a)</sup> Procedure as reported into the experimental section. General reaction conditions: Iodobenzene 0.25 mmol, Butylamine 0.625 mmol,  $\text{Cs}_2\text{CO}_3$  1 mmol, solvent 2 mL, T= 110 °C, time= 8 hours. <sup>b)</sup> Based on GC areas. <sup>c)</sup>  $\text{H}_2\text{O}/\text{CH}_3\text{CN} = 3/1$ . <sup>d)</sup> T= 80 °C.

<sup>e)</sup> T= 140 °C.

## Evaluation of TON and TOF values

Both turnover number (TON) and turnover frequency (TOF) values were used to compare the catalytic activity of the nanocomposite with analogous catalysts reported in the literature (Fig. 5 and Table 4). TON is defined as the number of moles of converted iodobenzene per mole of surface Cu (or Au) atoms (Fig. 5), while TOF is the number of moles of converted p-nitrophenol per mole of surface Cu (or Au) atoms per hour (Table 4).<sup>[ref. 14a]</sup> Although only a small portion of surface metal atoms can actually serve as catalytic active sites, some of them will be bonded to silicon structure and unavailable for catalysis, it is common to take the total number of surface atoms as the number of active catalytic sites when the value is not known [ref. 65].

Hence, in the case of TON values of Fig. 5, calculations were carried out as follows:

<p><i>Substrate:</i> iodobenzene (0,25 mmol),  <i>Conversion:</i> 96%,  <i>Catalyst:</i> CuNPs@SiNWs (1.5 µm, 1 cm<sup>2</sup>) [bearing <math>1.57 \times 10^{17}</math> Cu atoms/cm<sup>2</sup> (<math>1.67 \times 10^{-5}</math> g/cm<sup>2</sup>) which correspond to <math>2.61 \times 10^{-4}</math> mmol Cu/cm<sup>2</sup> (as resulted from Rutherford Backscattering Spectroscopy analyses)].</p> $\text{TON}_{\text{CuNPs@SiNWs}} = \frac{0.25 \times 0.96}{2.61 \times 10^{-4}} = 920$	<p><i>Substrate:</i> iodobenzene (0,25 mmol),  <i>Conversion:</i> 95%,  <i>Catalyst:</i> AuNPs@SiNWs (1.5 µm, 1 cm<sup>2</sup>) [bearing <math>1.95 \times 10^{17}</math> Au atoms/cm<sup>2</sup> (<math>6.41 \times 10^{-5}</math> g/cm<sup>2</sup>), which correspond to <math>3.24 \times 10^{-4}</math> mmol Au/cm<sup>2</sup> (as resulted from Rutherford Backscattering Spectroscopy analyses)].</p> $\text{TON}_{\text{AuNPs@SiNWs}} = \frac{0.25 \times 0.95}{3.24 \times 10^{-4}} = 736$
---	--

In the case of TOF values reported in Table 4, calculations were carried in a similar manner:

<p><i>Substrate:</i> 4-nitrophenol (0,05 mmol),  <i>Conversion:</i> 100%,  <i>Reaction time:</i> 1.5 h  <i>Catalyst:</i> CuNPs@SiNWs (1.5 µm, 0.5 cm<sup>2</sup>) which correspond to <math>1.31 \times 10^{-4}</math> mmolCu/cm<sup>2</sup></p> $\text{TOF}_{\text{CuNPs@SiNWs}} = \frac{0.05}{1.31 \times 10^{-4} \times 1.5} = 255 \text{ } h^{-1}$	<p><i>Substrate:</i> 4-nitrophenol (0,05 mmol),  <i>Conversion:</i> 100%,  <i>Reaction time:</i> 2.5 h  <i>Catalyst:</i> AuNPs@SiNWs (1.5 µm, 0.5 cm<sup>2</sup>) which correspond to <math>1.62 \times 10^{-4}</math> mmolAu/cm<sup>2</sup></p> $\text{TOF}_{\text{AuNPs@SiNWs}} = \frac{0.05}{1.62 \times 10^{-4} \times 2.5} = 123 \text{ } h^{-1}$
--	--

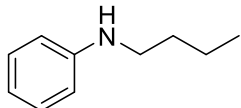
## **MS data of reaction products**

Reaction products were detected by GC–MS and identified by comparison of their MS spectra with the literature data. Below are reported both spectral experimental data and related literature:

### Caryl-N coupling products (table 1)

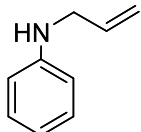
#### **N-butylaniline**

MS m/z (%): 149 (12, M<sup>+</sup>); 106 (100); 93 (3); 77 (14). Lit. [S1]



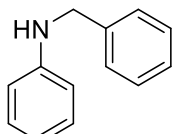
#### **N-allylaniline**

MS m/z (%): 133 (74, M<sup>+</sup>); 117 (22); 106 (100); 92 (12); 77 (46). Lit. [S2]



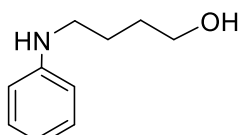
#### **N-benzylaniline**

MS m/z (%): 183 (40, M<sup>+</sup>); 106 (18); 91 (100); 77 (20). Lit. [S3]



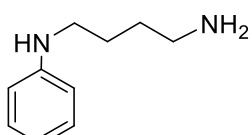
#### **4-(phenylamino)butan-1-ol**

MS m/z (%): 165 (11, M<sup>+</sup>); 106 (100); 93 (5); 77 (17). Lit. [S4]



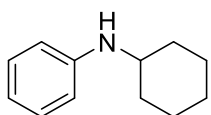
#### **N-(4-aminobutyl)benzenamine**

MS m/z (%): 164 (16, M<sup>+</sup>); 147 (6); 119 (10); 106 (100); 93 (20); 77 (28). Lit. [S5]



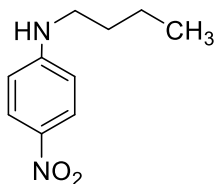
#### **N-cyclohexylaniline**

MS m/z (%): 175 (25, M<sup>+</sup>); 132 (100); 118 (20); 106 (12); 93 (18); 77 (16). Lit. [S6]



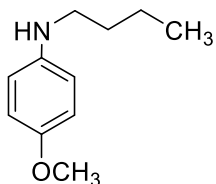
**N-butyl-4-nitroaniline**

MS m/z (%): 194 (20, M<sup>+</sup>); 151 (100); 135 (5); 121 (5); 105 (71); 77 (6). Lit. [S6]



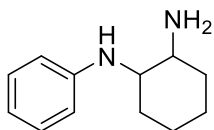
**N-butyl-4-methoxyaniline**

MS m/z (%): 179 (20, M<sup>+</sup>); 116 (100); 121 (5); 108 (8); 77 (5). Lit. [S6]



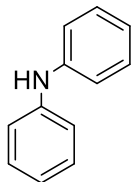
**N<sup>1</sup>-phenylcyclohexane-1,2-diamine**

MS m/z (%): 190 (55, M<sup>+</sup>); 172 (6); 147 (18); 132 (91); 118 (55); 106 (100); 97 (75); 77 (53). Lit. [S7]



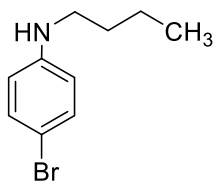
**Diphenylamine**

MS m/z (%): 169 (100, M<sup>+</sup>); 167 (31); 115 (6); 83 (24); 77 (18). Lit. [S8]



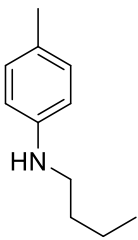
**4-bromo-N-butylaniline**

MS m/z (%): 228 (25, M<sup>+</sup>); 184 (100); 157 (5); 118 (10); 105 (50); 91 (15); 77 (15). Lit. [S9]



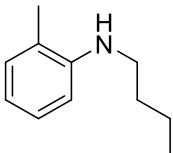
**N-butyl-4-methylaniline**

MS m/z (%): 163 (30, M<sup>+</sup>); 120 (100); 106 (5); 91 (25); 77 (12). Lit. [S9]



**N-butyl-2-methylaniline**

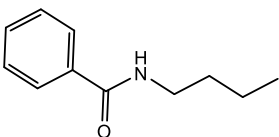
MS m/z (%): 163 (15, M<sup>+</sup>); 120 (100); 106 (5); 91 (15); 77 (5). Lit. [S9]



Aminocarbonylation products (table 2)

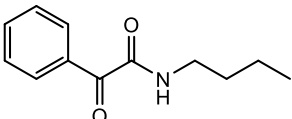
**N-butylbenzamide**

MS m/z (%): 177 (10, M<sup>+</sup>); 135 (25); 105 (100); 77 (66). Lit. [S10]



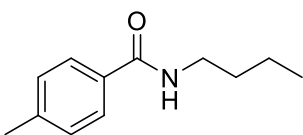
**N-butyl-2-oxo-2-phenylacetamide**

MS m/z (%): 205 (9, M<sup>+</sup>); 105 (100); 77 (45); 57 (40). Lit. [S11]



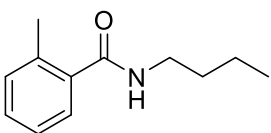
**N-butyl-4-methylbenzamide**

MS m/z (%): 191 (10, M<sup>+</sup>); 148 (12); 119 (100); 91 (25). Lit. [S11]



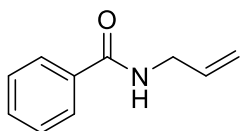
**N-butyl-2-methylbenzamide**

MS m/z (%): 191 (14, M<sup>+</sup>); 148 (7); 176 (<5); 119 (100); 91 (50); 65 (25). Lit. [S11]



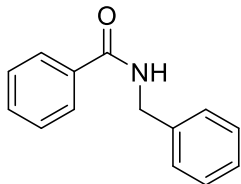
**N-allylbenzamide**

MS m/z (%): 161 (8, M<sup>+</sup>); 146 (8); 105 (100); 94 (12); 77 (52). Lit. [S12]



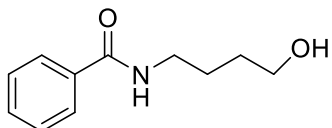
**N-benzylbenzamide**

MS m/z (%): 211 (50, M<sup>+</sup>); 177 (10); 167 (5); 135 (10); 105 (100); 91 (18); 77 (60). Lit. [12]



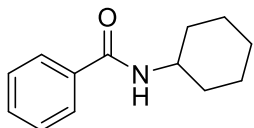
**N-(4-hydroxybutyl)benzamide**

MS m/z (%): 193 (10, M<sup>+</sup>); 162 (5); 148 (15); 134 (10); 105 (100); 91 (18); 77 (50). Lit. [S13]



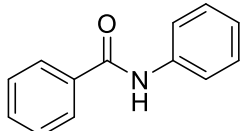
**N-cyclohexylbenzamide**

MS m/z (%): 203 (23, M<sup>+</sup>); 160 (5); 122 (70); 105 (100); 77 (55). Lit. [S14]



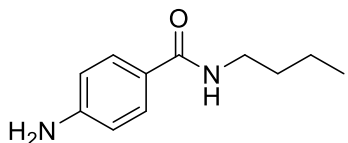
**N-phenylbenzamide**

MS m/z (%): 197 (30, M<sup>+</sup>); 105 (100); 77 (60). Lit. [S14]



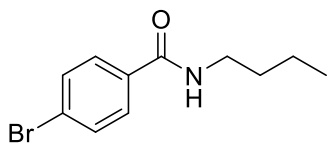
**4-amino-N-butylbenzamide**

MS m/z (%): 192 (12, M<sup>+</sup>); 120 (100); 92 (20); 65 (22). Lit. [S15]



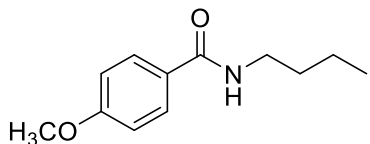
**4-bromo-N-butylbenzamide**

MS m/z (%): 257 (16, M<sup>+</sup>); 255 (15, M<sup>+</sup>); 213 (20); 185 (100); 157 (20); 104 (10); 76 (30). Lit. [S16]



**N-butyl-4-methoxybenzamide**

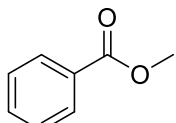
MS m/z (%): 207 (15,  $\text{M}^+$ ); 164 (15); 135 (100); 107 (10); 92 (14); 77 (18). Lit. [S17]



Alkoxy carbonylation products (table 3)

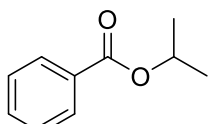
**Methyl benzoate**

MS m/z (%): 136 (27,  $\text{M}^+$ ); 105 (100); 92 (5); 77 (65). Lit. [S12]



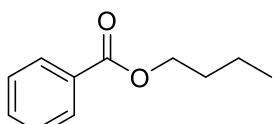
**Isopropyl benzoate**

MS m/z (%): 164 (7,  $\text{M}^+$ ); 146 (5); 122 (34); 105 (100); 77 (45). Lit. [S12]



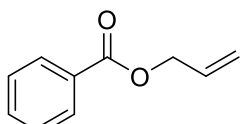
**Butyl benzoate**

MS m/z (%): 178 (<5,  $\text{M}^+$ ); 123 (65); 105 (100); 91 (<5); 77 (65); 56 (25). Lit. [S18]



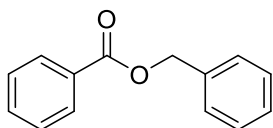
**Allyl benzoate**

MS m/z (%): 162 (5,  $\text{M}^+$ ); 117 (4); 105 (100); 77 (47). Lit. [S19]



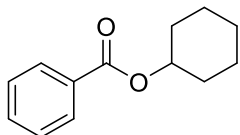
**benzyl benzoate**

MS m/z (%): 212 (10,  $\text{M}^+$ ); 194 (5); 105 (100); 91 (70); 77 (50). Lit. [S14]



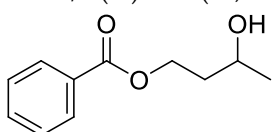
### cyclohexyl benzoate

MS m/z (%): 204 (<5, M<sup>+</sup>); 123 (90); 105 (100); 77 (50); 67 (40). Lit. [S12]



### 3-hydroxybutyl benzoate

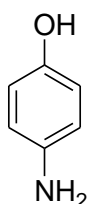
MS m/z (%): 194 (<5, M<sup>+</sup>); 149 (10); 123 (40); 105 (100); 77 (60). Lit. [S20]



### Reduction products (table 4 and Fig. 7)

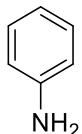
#### 4-aminophenol

MS m/z (%): 109 (100, M<sup>+</sup>); 96 (5); 80 (82); 77 (10). Lit. [S21]



### Aniline

MS m/z (%): 98 (100, M<sup>+</sup>); 66 (55). Lit. [S21]



### References

- S1 Li, Y.-Q.; Chen, Y.-B.; Huang, Z.-Z. *Chinese Chemical Letters* **2014**, *25*, 1540–1544.
- S2 Ohshima, T.; Miyamoto, Y.; Ipposhi, J.; Nakahara, Y.; Utsunomiya, M.; Mashima, K. *J. Am. Chem. Soc.* **2009**, *131*, 14317–14328.
- S3 Zhang, G.; Scott, B. L.; Hanson, S. K. *Angew. Chem. Int. Ed.* **2012**, *51*, 12102 –12106.
- S4 Compared with: [https://www.chemsrc.com/en/Spectral/6517-80-2\\_1180315.html](https://www.chemsrc.com/en/Spectral/6517-80-2_1180315.html)
- S5 Ramirez, M. A.; Corona, M. V.; Blanco, M. M.; Perillo, I. A.; Porcal, W.; Salerno A. *Tetrahedron Lett* **2010**, *51*, 5000–5002
- S6 Huang, L.; Yu, R.; Zhu, X.; Wan, Y. *Tetrahedron* **2013**, *69*, 8947-8977.
- S7 Egli, v. M.; Hoesch, L.; Dreiding, A. S. *Helvetica Chimica Acta*, **1985** Vol. 68.

- S8 Huang, L.; Yu, R.; Zhu, X.; Wan, Y. *Tetrahedron* **2013**, *69*, 8974-8977.
- S9 Castillo, J.-C.; Orrego-Hernandez, J.; Portilla, J. *Eu. J. Org. Chem.* **2016**, *22*, 3824–3835.
- S10 Li, Y.; Chen, H.; Liu, J.; Wan, X.; Xu, Q. *Green Chem.*, **2016**, *18*, 4865-4870.
- S11 Marosvolgyi-Hasko, D.; Kegl, T.; Kollar, L. *Tetrahedron* **2016**, *72*, 7509-7516.
- S12 Mane, R. S.; Sasaki, T.; Bhanage, B. M. *RSC Adv.*, **2015**, *5*, 94776.
- S13 Petersson, M. J.; Jenkins, I. D.; Loughlin, W. A. *Org. Biomol. Chem.*, **2009**, *7*, 739-746.
- S14 Khedkarte, M. V.; Sasaki, T.; Bhanage, B. M. *ACS Catal.* **2013**, *3*, 287-293.
- S15 Wang, Y.; Wu, Z.; Li, Q.; Zhu, B.; Yu, L. *Catal. Sci. Technol.*, **2017**, *7*, 3747-3757.
- S16 Shen, C.; Wei, Z.; Jiao, H.; Wu, X.-F. *Chem. Eur. J.* **2017**, *23*, 13369 –13378.
- S17 Fang, T.; Gao, X.-H.; Tang, R.-Y.; Zhang, X.-G.; Deng, C.-L. *Chem. Commun.*, **2014**, *50*, 14775-14777.
- S18 Gayakwad, E. M.; Patil, V. V.; Shankaarling, G. S. *New J. Chem.* **2017**, *41*, 2695-2701.
- S19 Hemming, D. S.; Talbot, E. P.; Steel, P. G. *Tetrahedron lett.*, **2017**, *58*, 17-20.
- S20 Hungerbühler, E.; Seebach, D.; Wasmuth, D. *Helvetica Chimica Acta* **1981**, *64*, 1467 – 1487.
- S21 NIST Database and comparison with authentic sample.